AIAA SciTech Forum
12-16 January 2026, Orlando, FL
AIAA SCITECH 2026 Forum

10.2514/6.2026-2133

A Method for Charge Exchange Corrections for Hall Thruster Plumes

Madison G. Allen* and Benjamin Jorns†
University of Michigan, Ann Arbor, MI, 48109

The various charge exchange correction methods for a Hall effect thruster's ion current density profile are investigated and compared. This study is conducted on the HERMeS thruster plume profiles at 300V 6.25kW and 600V 12.5kW. An additional method is proposed that leverages ion energy distribution data to determine the charge exchange contribution across the plume and introduces a factor for particle attenuation. The model is compared to the thruster profile achieved using the best practices approach. The resulting profile showed improved agreement at large angles of the plume for the 600V condition. This method offers a simple, physics-based profile estimation for improved plume characterization.

I. Introduction

Hall effect thrusters have historically been implemented on spacecrafts for orbit raising, station-keeping, and more recently, long duration, deep-space missions [1, 2]. Despite the widespread success of this technology, there is an ongoing challenge with these systems where ground testing thruster operation has been shown to diverge from "on-orbit" operation. This discrepancy is believed to in part be a result of the ground testing facility's limited pumping speeds [3]. Consequently, the background pressure in a vacuum chamber is generally greater than the space environment causing a thruster response to the large presence of neutrals. Examples of these behavior changes include overall performance i.e. thrust, as well plume oscillations. The thruster plume will also experience changes in current and its structure [4–12].

One of the key facility effects is charge exchange collisions. These collisions occur when a high energy ion interacts with a low energy neutral and trades an electron resulting in a low energy ion and high energy neutral [13, 14]. These neutrals are typically due to the facility's inability to remove all of the background gas particles. The charge exchange ions can experience strong radial electric fields that artificially increases the current found at large angles in the plume. This impacts current density profiles and displays false characteristics such as larger plume divergence. Researchers often will employ experimental methods to correctly ascertain the plume profile by measuring multiple probe traces at different radial positions or facility background pressures [15, 16]. These methods tend to be experimentally expensive with larger operation time and cost. As a more cost-effective approach, researchers will analytically correct the thruster plume profile from a single probe trace during post-processing. These methods require assumptions to be made for the plume that may not be suitable for all devices. Thus there is an apparent need for a correction method that accurately accounts for charge exchange effects using actual plume information. This work investigates the use of ion energy distribution functions to determine the charge exchange current contribution to the total current measured across the plume as well as a correction for the particle attenuation.

This paper is organized in the following way. In Section 2, we first describe the ion current density profile and various methods for charge exchange corrections currently established in the community. We also include the proposed method using ion energy distributions. We introduce the dataset including the thruster, HERMeS, and diagnostics used. We then present the results with a comparison of the methods, in Section 3. In Section 4, we discuss our findings as well as some of the limitations to this additional approach.

II. Methodology

In this section we first introduce the current density profile and discuss its characteristics as well as the experimental procedure for profile acquisition. We then provide the different methods within the electric propulsion community to adjust for charge exchange effects and the method proposed in this work. Finally, we present the dataset used in this work.

*PhD Candidate, Aerospace Engineering
†Associate Professor, Aerospace Engineering

A. Current Density Profiles

Current density profiles often provide key information for understanding thruster performance. With these profiles, we can determine thruster characteristics such as the plume's divergence from the thrust vector as well as the total amount of current carried by the plume. We briefly review here the ion populations typically found in a Hall thruster plume [17, 18].

There exist main beam ions born in the thruster channel via neutral-electron ionization with predominantly axial velocity. These ions will interact with background neutrals from the facility as well as neutrals from unionized propellant. This interaction can be an elastic scattering where the ion retains most of its energy but may change direction causing a plume expansion [19]. There can also be ions born due to charge exchange of an accelerated ion and slow neutral, as previously mentioned. They are predominantly found at angles greater then 70 degrees[19]. Charge exchange can occur symmetrically ($A^+(fast) + A(slow) \rightarrow A(fast) + A^+(slow)$ or $A^{2+}(fast) + A(slow) \rightarrow A(fast) + A^{2+}(slow)$) or asymmetrically ($A^{2+}(fast) + A(slow) \rightarrow A^+(fast) + A^+(slow)$) [20, 21]. In this work, we account for singly charged symmetric charge exchange. We base this off of the fact that the Hall thruster plume mainly consists of singly charged ions.

When measuring the ion current density of a Hall effect thruster, a probe is swept in a typically hemispherical coordinate system maintaining a constant radial distance about the center of the thruster face. The recommended diagnostic is a Faraday probe where the probe is biased negatively such that the collected current is from the ion saturation regime. The probe will create a sheath that allows the probe current collected to include the Bohm current. The probe measures current collected at small angular intervals across the expanse of the thruster ($-90°$, $90°$). The ion current density is then calculated with $j_{FP}(r, \theta) = I_{FP}(r, \theta)/A$ where the radial distance from the thruster is r, angular position from centerline is θ, I is the collected current, and A is the probe area. We note here that there are additional corrections employed to account for the probe geometry, channel ion trajectories, and secondary electron emissions [16].

As the plume propagates downstream, the ions will continue to experience neutral interaction which results in a probe measured plume that is a misrepresentation of the plume at the thruster face that accurately demonstrates thruster performance. This is strongly due to the additional current in the periphery of the plume as a result of charge exchange ions. This is exacerbated with the measured Bohm current falsely increasing the amount of beam current present.

B. Best practices for current density correction

To deconvolve the effects of charge exchange of Bohm current, the experimental method that is best practice is to take multiple Faraday probe traces at various radial positions (Fig. 1a). If we perform a linear fit to the current density data at a single angular position, we can extrapolate to $r = 0$ at the thruster face and achieve a representative plume profile [15, 16]. This provides a profile that does not contain any facility neutral interaction or attenuation that occurs in the region between the thruster face and far-field probe. We note it is also recommended for on-orbit plume predictions to perform Faraday probe sweeps at various background pressure conditions and perform a similar parametric fit and subsequent extrapolation. While these methods are appropriate in theory, the challenge in practice is that can be experimentally expensive to perform this many traces. Due to experiment limitations, such as space, time or equipment restrictions, it may be impractical to perform this method. However, researchers have implemented various other simple, analytical charge exchange current corrections.

C. Correction Methods

We present here multiple methods for correcting for charge exchange current in ion current density traces taken at a radial point. These attempts rely on one Faraday probe trace. We start with a simple model for the current density collected by the probe:

$$j_{FP}(r, \theta) = j_{beam}(r, \theta) + j_{CEx,Bohm}(r, \theta). \tag{1}$$

Here j_{FP} is the current density measured by the probe, j_{beam} is the ion beam plume current, $j_{CEx,Bohm}$ is the current we correct. The goal in practice then is to develop models for how to account for this latter term in order to arrive at an approximation for the true current at the thruster exit.

1. Flat subtraction

The first method is to subtract the minimum current density off of the entire profile [22]. This assumes that the current at about 90 degrees is solely made up of charge exchange ions. This method also assumes that the charge

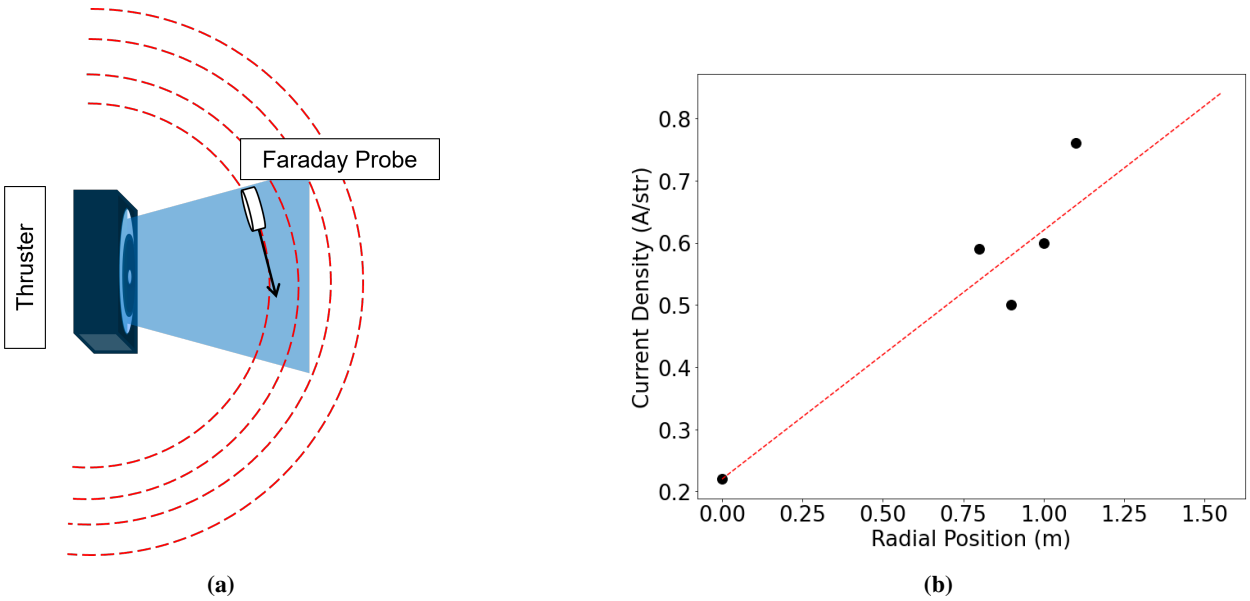

(a) **(b)**

Fig. 1 a.) A drawing of a Hall thruster and Faraday probe with an example of the multiple sweep paths. b.) An example plot of the resulting data and extrapolation at one angle.

exchange contribution is independent of angle. This can be represented by

$$j_{CEx,Bohm}\left(r,\theta\right) = \min\left(j\left(r,\theta\right)\right). \tag{2}$$

In practice, the minimum measurement is typically at the 90° position. According to ion energy distribution profiles, there is an angular dependence for charge exchange ions, such that this method generally underpredicts charge exchange current.

2. Model fits

The next two methods are similar in that they assume that the ion beam profile follows some known functional form, i.e. an exponential or Gaussian curve [15][17]. This typically requires fitting to the near centerline regions and extrapolating to the larger angles. The exponential method fits to current density from approximately 15° to 40° off centerline on each side of the plume [23]:

$$j_{beam} = ae^{-b\theta}, \tag{3}$$

where a, b are fitting parameters. The Gaussian is fit to the region from −40° to 40°:

$$j_{beam} = ae^{-(\theta-b)^2/c^2}, \tag{4}$$

where c is an additional fitting parameter. The model fit methods assume that any thruster plume profile follows this trend. The drawback is that this may not be true or valid–particularly given that these fit functions are phenomenologically motivated. In practice, results for corrected current densities with this approach tend to overpredict the charge exchange effect.

3. Proposed retarding potential Analyzer correction

The new method we propose is to leverage ion energy distribution profiles to determine the ratio of current from a charge exchange contribution to the total current at various angles. This ratio is then applied to the Faraday probe current density value at each angle. The ion energy data is measured using a retarding potential analyzer, which assesses I-V traces by biasing an ion suppression grid. By sweeping this voltage and collecting the varying current an ion energy distribution can be determined. Provided we have this assessment, the proposed correction per method is

$$j_{beam}\left(r,\theta\right) = j_{FP}\left(r,\theta\right)\left(1 - \frac{I_{RPA,CEx}(r,\theta)}{I_{RPA}(r,\theta)}\right), \tag{5}$$

where $I_{RPA,CEX}$ is the charge exchange current and I_{RPA} is the total RPA current. The charge exchange current is assumed to be any current that is found at energies less than 15% of the discharge voltage [19].

4. Plume attenuation correction

Regardless of our correction method, once we have an estimate for the beam current density at a fixed radial location, $j_{beam}(r, \theta)$, we also need to account for plume attenuation of this beam. This stems from the fact that a fraction of this current is lost to charge exchange effects. To motivate this, we consider the continuity equation for all ions originating from the thruster channel:

$$\frac{\partial n_i}{\partial t} + \nabla \cdot [n_i \vec{u}_i] = -n_n \sigma_{CEX} n_i |\vec{u}_i|, \tag{6}$$

where n_i is the local ion density, n_n denotes the local neutral density, u_i is the ion velocity, and σ_{CEX} is the charge exchange collisional cross-section. In this equation, the right hand side represents a loss term for ions lost to charge exchange collisions. If we assume that the system is at steady state and the flux of ions is only non-uniform in the radial direction in spherical coordinates, we arrive at

$$\frac{1}{r}\frac{\partial}{\partial r} r n_i u_i = -n_n(r)\sigma_{CEX}(\theta) n_i u_i. \tag{7}$$

In order to model the neutral density in the thruster plume, we allow for both background effects and neutrals stemming from unionized propellant exiting the channel: $n_n(r) = n_{n,background} + n_{n,propellant}(r)$. The neutral density due to the background pressure in the facility is assumed constant, but the propellant neutrals have some bulk velocity supplied at the thruster and propagate radially upon exiting. They also expand spherically. We thus represent $n_{n,propellant}(r) = n_{n,propellant}(0) A_{ch}/2\pi r^2$, where A_{ch} denotes the area of the channel. Additionally, the charge exchange collisional cross-section is dependent on ion energy which varies as a function of angle [20, 21]. Armed with this result, we use it jointly with Eq. 7 to find the ion beam as a function of radial position and neutral density:

$$j_{beam}(r = 0, \theta) = j_{beam}(r = r, \theta) \exp\left(n_{n,b}\sigma_{CEX}(\theta) r - \frac{n_{n,p}(0) A_{ch}}{2\pi r}\sigma_{CEX}(\theta)\right). \tag{8}$$

D. Test Case

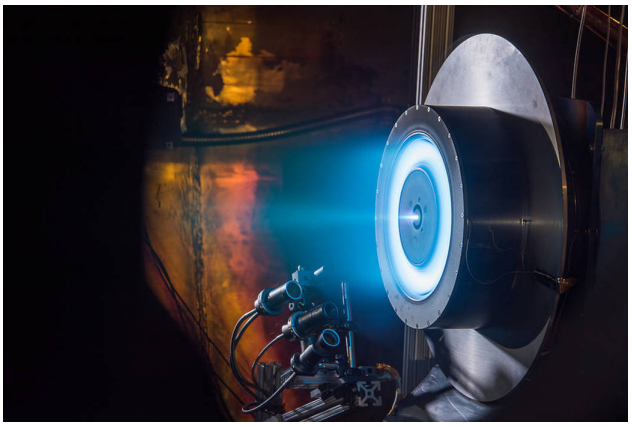

Fig. 2 Image of HERMeS operating [24]

In this section we overview the current density and ion energy distribution datasets we used to evaluate the different methods. These stem from the work published by Huang et al. [25] on the HERMeS thruster. The HERMeS engine (Fig. 2) is a magnetically shielded Hall effect thruster with an internally mounted cathode. The thruster was configured with the thruster body grounded and a graphite pole cover. The thruster was tested at NASA GRC in VF5 at 300V 6.25kW and 600V 12.5kW on xenon. VF5 is a 4.6 m by 18.3 m vacuum testing facility with cryopanels that achieve an operating background pressure for both conditions of 4.2 μTorr. During this test, a Faraday probe and retarding potential analyzer (RPA) were mounted on motion stages to allow rotational motion about the thruster and radial translation from

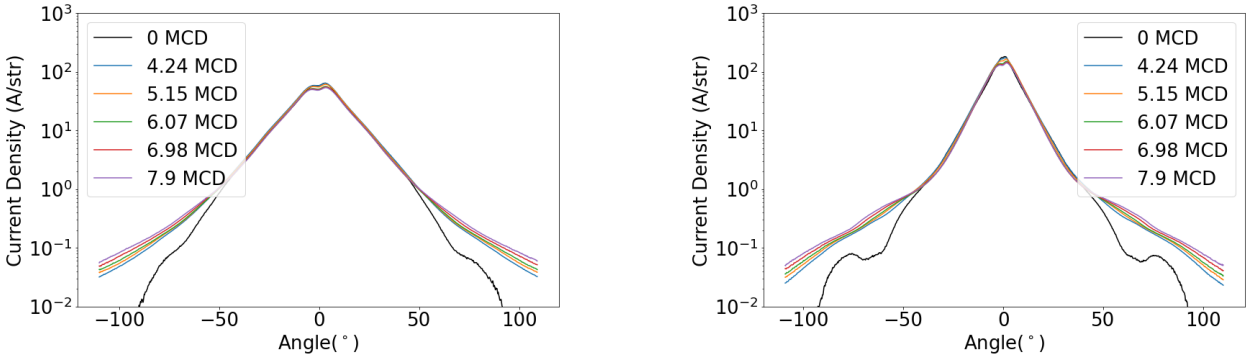

(a) **(b)**

Fig. 3 A plot of the ion current density profiles at six distances for the a.) 300V 6.25kW and b.) 600V 12.5kW conditions.

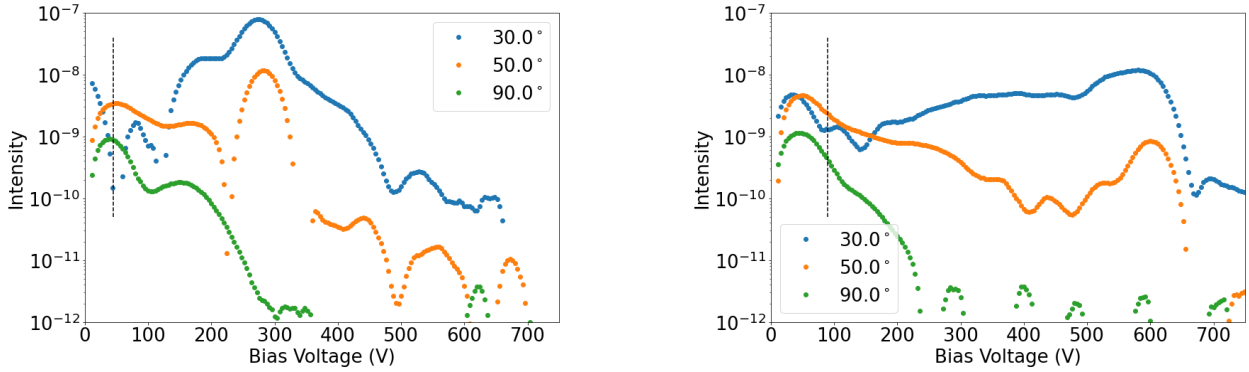

(a) **(b)**

Fig. 4 A plot of ion energy distributions for three different angles in the plume at the a.) 300V 6.25kW and b.) 600V 12.5kW condition.

the thruster to investigate the plume profile. The GRC guarded Faraday probe was swept across the plume from −110° to 110° at 5 radial distances to collect ion current density measurements. In Figure 3, we plot the radial profiles as well as the extrapolated 0 MCD profile for both operating conditions. The MCD refers to the mean channel diameter and serves as a scaling parameter. The current density profile at 0 MCD represents the plasma plume at the thruster exit assuming no attenuation or facility charge exchange. The AFRL RPA was a four grid design (floating, electron suppression, ion suppression, electron repelling) and was swept from −105° to 105°. I-V curves were collected at close to the 7.9 MCD radial position from the thruster. The ion energy distributions were determined using the relationship $\frac{dI}{dV} \propto f(E/q)$. We provide an example of the IEDFs used in Figure 4 as well as a vertical line demonstrating the voltage we use to identify charge exchange current energy limit. In the next section we present the results when the correction methods were applied to this dataset.

III. Results

In this section, we present the results of the charge exchange corrections: subtraction, functional fits (Gaussian and exponential) and RPA correction for the two HERMeS operating conditions. We applied each correction method to the 7.9 MCD ion current density trace and plotted the results in Figure 5. We note here that to accurately compare the different adjustments we employed the RPA correction method without the particle attenuation factor using Equation 5. The goal of these correction methods is to produce a comparable result to the extrapolated 0 MCD profile. To do so, we account for the attenuation of the plume as it travels downstream. We compared the extrapolated 0 MCD result to the RPA correction with the particle attenuation factor from Equation 8 in Figures 6 and 7.

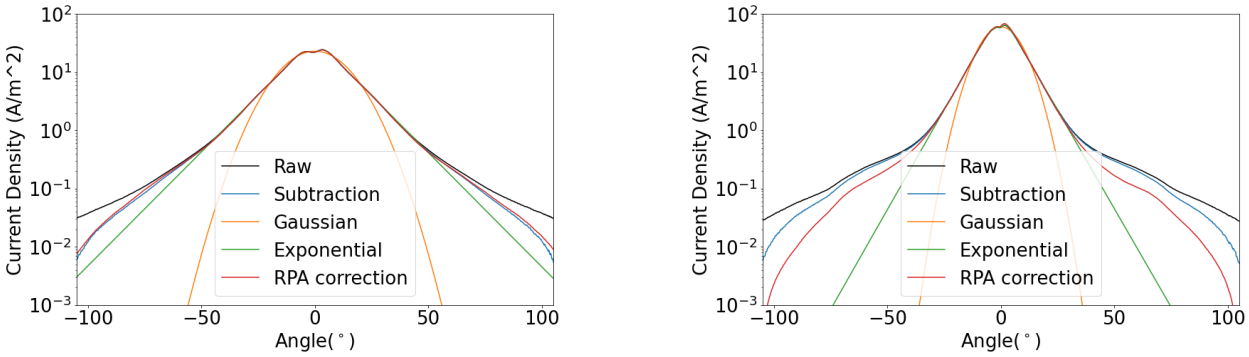

Fig. 5 A plot of the ion current density with the various charge exchange corrections at 7.9 MCD at the a.) 300V 6.25kW and b.) 600V 12.5kW condition.

A. 300V 6.25kW

From Figure 5a, the subtraction approach shows a substantive effect at only the large angles of the plume. The result is fairly linear and comparable to the exponential fit, but the exponential fit assumes a larger charge exchange presence. With the Gaussian we are fitting strictly to the ion beam region near centerline. As a result, the elastically scattered ion contribution is removed from the profile as well as the charge exchange current. Interestingly, the RPA correction is comparable to the subtraction method where the charge exchange contribution is only in the wings of the plume. From this result, we can potentially assume that the RPA correction factor assumes charge exchange is independent of angle at this condition. In Figure 6a, the extrapolated result demonstrates that the RPA correction is not capturing all of the charge exchange current. It also does not represent the profile shape accurately. The potential causes of this discrepancy is that the 15% approximation does not capture the full charge exchange energy. The charge exchange energy distribution could have a fast ion tail that is outside of the 15% of the discharge voltage set energy limit. If we view the result in a linear scale (Fig. 7a), there is also content that the attenuation factor is not accounting for correctly near the centerline.

B. 600V 12.5kW

From Figure 5b, the subtraction method again shows its largest change in the periphery of the plume. Additionally, the interesting contours of the profile shape remain with a flat subtraction. This cannot be said when applying a functional fit. We see that the functional fits remove much of the current at large angles. The Gaussian and exponential fits both seem to remove current from elastically scattered ions, unlike the 300V exponential correction. All of the characteristics in the profile shape are ignored when the functional fits are employed. The subtraction scheme presents an improvement in that it maintains the profile shape. The RPA correction exhibits even more of these contours where it also shows a large deviation from the subtraction method. It has a magnitude between that of the subtraction and exponential methods. It assumes more charge exchange presence than subtraction but less charge exchange contribution than the exponential fit. When we compare to the extrapolated result in Figure 6b, we find an improved result than the 300V condition. The main difference is that the RPA correction misses peaks seen at approximately ±80°. The linearly scaled result (Fig. 7b), once again shows that the attenuation factor is not capturing the total current near centerline.

IV. Discussion

In this section, we discuss the implications of this study as well as some provide the results when adjusting the original assumptions. We then mention limitations to the RPA correction method.

A. Implications

In this study, we proposed a method for correcting for charge exchange using the ion energy distribution data from a retarding potential analyzer. We performed the correction procedure on the operating conditions for the HERMeS thruster. While the discharge voltages differed, the discharge current was held constant. This difference is evident in the plume profiles such that the wings of the profile are more exaggerated in the 600V profile. There is a distinct separation

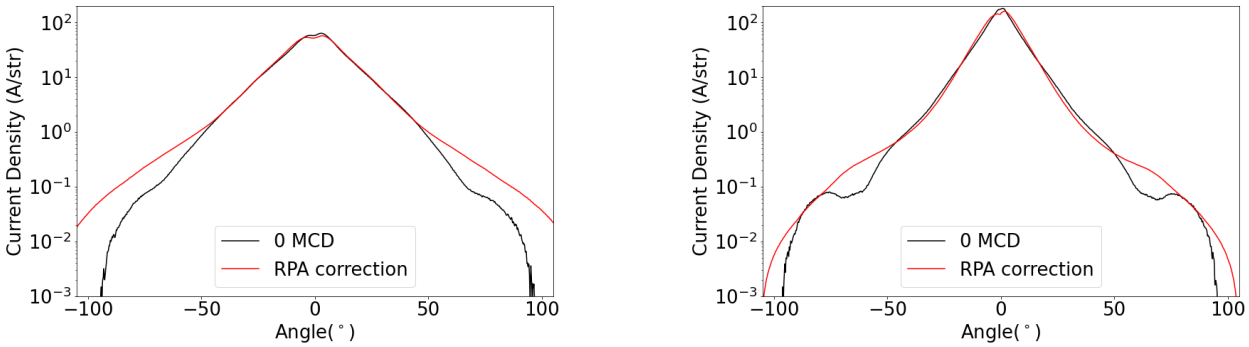

Fig. 6 A plot the of log scale ion current density comparing the 0 MCD extrapolated profile to the 7.9 MCD RPA corrected profile at the a.) 300V 6.25kW and b.) 600V 12.5kW condition.

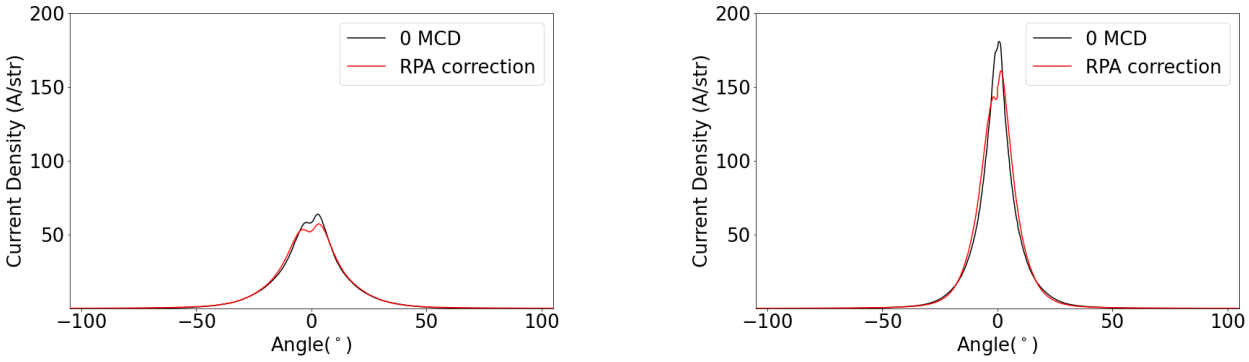

Fig. 7 A plot of the linear scale ion current density comparing the 0 MCD extrapolated profile to the 7.9 MCD RPA corrected profile at the a.) 300V 6.25kW and b.) 600V 12.5kW condition.

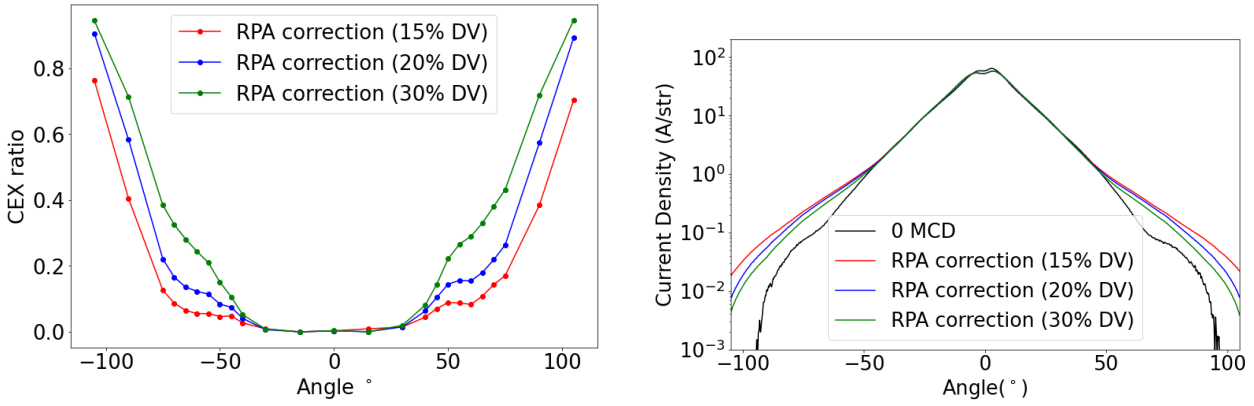

(a) **(b)**

Fig. 8 a.) A plot of the ratio of charge exchange current against total current assuming a charge exchange energy of 15%, 20%, and 30% of the discharge voltage. b.) A plot of the ion current density as a function of angle for the 0 MCD trace and the RPA Correction for varying energy limit percentages of the discharge voltage at 300V 6.25kW.

between the collimated beam ions and the scattered or charge exchange ions. This could be due to the fact that there is a smaller collisional cross-section thus a lower probability or larger mean free path for ion-neutral interactions with larger ion energy [21]. The large distinction causes the functional fit methods to be a poor substitute especially at 600V. With that, the RPA correction shows better agreement to the extrapolated profile for the 600V case than the 300V case. This could be due to the fact that ions of higher energies are accepted with the 15% of the discharge voltage set as the energy limit for the 600V profile. In the next section, we show results when the energy limit is adjusted. Briefly, we note that the results demonstrated the RPA correction was similar to the flat subtraction approach for the 300V condition, but similar to the average of the flat subtraction and exponential function for the 600V condition. This is specifically beneficial to experiments that are limited to one probe diagnostic (a Faraday probe) at one radial distance.

We now comment on the current discrepancy along centerline. When incorporating the evaluated particle attenuation in Equation 8, the current increase is around 10%. For the particle attenuation to achieve the expected current, the pressure will need to be approximately twice the measured value. A potential cause of this discrepancy is that we did not account for the displacement when ions are elastically scattered. If we assume the same cross-sectional area as the charge exchange interactions, then this could account for the missing factor of two. This would require correction for these ions as well. If the ion energy distributions were used to determine elastically scattered ion current, it would be generally more difficult due to the large expanse of energies for this ion population's distribution. In this work, the goal was to suggest another method for correcting charge exchange interactions, but to accurately depict the plume profile at the thruster we will need to account for the elastic scattering of ions.

B. Further Investigations

For the RPA correction method, we assumed that charge exchange current only existed at energy levels below 15% of the discharge voltage. To investigate this assumption, we plotted the ratio of charge exchange as a function of angular position for three slightly different energy limits– 15%, 20%, and 30% of the discharge voltage –for the 300V condition in Figure 8a. The results show that there is a significant amount of current near this region of energy limits. Specifically at the furthest angles from centerline, there is a large current increase from 15% to 20% in comparison to the 20% to 30% transition. This further illustrates that we are cutting off current at the peak of the distribution, as does the example ion energy distributions presented in Figure 3a. This current could be charge exchange that we are neglecting to account for due to an inaccurate assumption for this particular thruster. We also plotted the ion current density for the two different percentages for the 600V condition in Figure 9b and found better agreement at 20% of the discharge voltage. Once again, the contours are not present, but the average magnitude over that region is similar to the 20% attempt. The 30% energy limit is not shown but over corrects for charge exchange. We may have been removing propellant neutral charge exchange or other populations of ions that are not due to the facility neutral interactions with the 30% case.

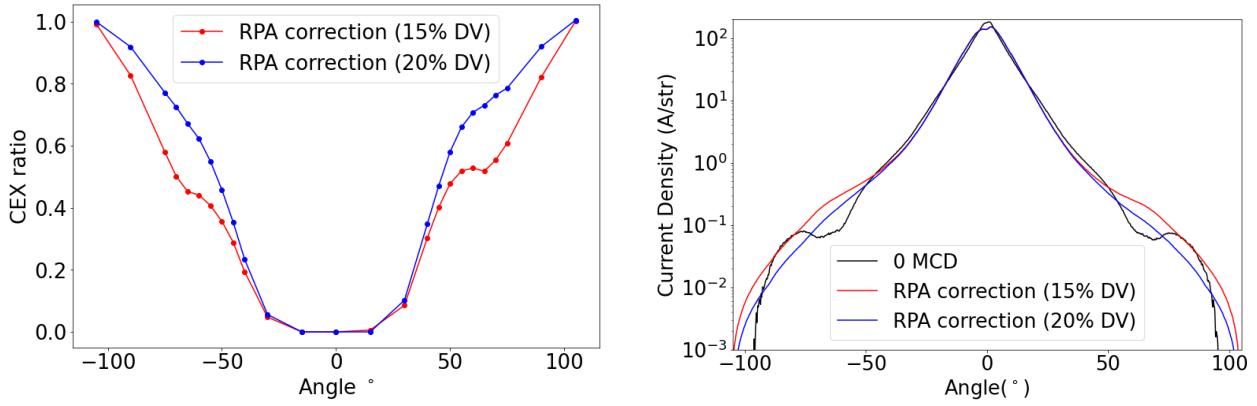

(a) **(b)**

Fig. 9 a.) A plot of the ratio of charge exchange current against total current assuming a charge exchange energy of 15% and 20% of the discharge voltage. b.) A plot of the ion current density as a function of angle for the 0 MCD trace and the RPA Correction for varying energy limit percentages of the discharge voltage at 600V 12.5kW.

C. Limitations

For this method, we attempted to remove all of the charge exchange contribution due to the facility. By applying a strict energy limit, we may additionally be removing charge exchange due to interactions with propellant neutrals. These neutrals are a result of thruster inefficiency and are unrelated to charge exchange as a facility effect. An improvement would be to identify a way to distinguish between facility charge exchange and propellant charge exchange. Additionally, we are neglecting the interactions with and current provided by multiply charged species. Multiply charged species also have charge exchange interactions and these charge exchange ions would be seen at higher energies in the ion energy distributions. Another limitation to the model is the incomplete ion energy distributions. Since the cathode potential typically floats below ground and the probe was biased with respect to ground there is potentially content the distributions are not capturing. This could be described analytically as

$$\frac{I_{RPA,CEx}(r,\theta) + I_{V_{c2g}<V<0}}{I_{RPA}(r,\theta) + I_{V_{c2g}<V<0}}. \tag{9}$$

Lastly, we briefly mention collimated versus uncollimated probes. Because the Faraday probe used in this study is uncollimated, it can collect current offset from its normal trajectory. This is unlike the collimated RPA where ions slightly off axis can be lost to the walls of the probe. Generally retarding potential analyzers collect less current than the Faraday probe, but they also may be biased to blocking more of the charge exchange ions from reaching the collector.

V. Conclusion

Hall thruster plume profiles are an effective way to improve overall understanding of thruster performance or near-surface interactions. Yet, the presence of charge exchange due to the testing facility background pressure impacts the measured profile. In this work, we presented a method for correcting ion current density profiles for charge exchange. Previous methods have been proposed that can misrepresent the plume profile. While the preferred method is to perform multiple radial traces, this may be impractical for certain facilities. The proposed method relies on ion energy distributions provided by a Retarding Potential Analyzer. This approach was applied to a HERMeS dataset and demonstrated agreement in the large angles of the plume for the high voltage condition. The agreement improved for the low voltage condition when the approach assumptions were relaxed. Unfortunately, work needs to continue on the plume attenuation adjustment. This technique may not fully capture the profile but offers a step towards better agreement. Future work is to apply this method to various thruster plumes to determine the accuracy of the method, as well as utilize the plume estimation for thruster performance evaluation.

Acknowledgments

The authors would like to thank the NASA Space Technology Research Opportunity, Grant 80NSSC22K1172, as well as the NASA Research Institute, the Joint AdvaNced propUlsion inStitute (JANUS), for supporting this work. The authors would also like to thank Dr. Wensheng Huang for providing the datasets.

References

[1] Snyder, J. S., Goebel, D. M., Ortega, A. L., Mikellides, I. G., Aghazadeh, F., Johnson, I., and Lenguito, G., "Electric Propulsion for the Psyche Mission," *36th International Electric Propulsion Conference*, 2019, p. 244.

[2] Herman, D. A., Tofil, T. A., Santiago, W., Kamhawi, H., Polk, J. E., Snyder, J. S., Hofer, R. R., Picha, F. Q., Jackson, J., and Allen, M., "Overview of the Development and Mission Application of the Advanced Electric Propulsion System (AEPS)," *International Electric Propulsion Conference*, 2017.

[3] Randolph, T., Kim, V., Kaufman, H., Kozubsky, K., Zhurin, V., and Day, M., "Facility Effects on Stationary Plasma Thruster Testing," *Proceedings of the 23rd International Electric Propulsion Conference*, 1993.

[4] Hofer, R. R., Peterson, P., and Gallimore, A., "Characterizing Vacuum Facility Backpressure Effects on the Performance of a Hall Thruster," *27th International Electric Propulsion Conference*, 2001, pp. IEPC–01–045. URL `http://adsabs.harvard.edu/abs/2005PhDT.....46W`.

[5] Walker, M. L., Victor, A. L., Hofer, R. R., and Gallimore, A. D., "Effect of backpressure on ion current density measurements in hall thruster plumes," *Journal of Propulsion and Power*, Vol. 21, 2005, pp. 408–415. https://doi.org/10.2514/1.7713.

[6] Byers, D., and Dankanich, J., "A Review of Facility Effects on Hall Effect Thrusters," *31st International Electric Propulsion Conference*, 2009. URL http://erps.spacegrant.org/uploads/images/images/iepc_articledownload_1988-2007/2009index/IEPC-2009-076.pdf.

[7] Diamant, K. D., Liang, R., and Corey, R. L., "The Effect of Background Pressure on SPT-100 Hall Thruster Performance," *50th AIAA/ASME/SAE/ASEE Joint Propulsion Conference*, American Institute of Aeronautics and Astronautics, 2014. https://doi.org/10.2514/6.2014-3710.

[8] Huang, W., Kamhawi, H., Lobbia, R. B., and Brown, D. L., "Effect of background pressure on the plasma oscillation characteristics of the HiVHAc Hall thruster," *50th AIAA/ASME/SAE/ASEE Joint Propulsion Conference 2014*, 2014, pp. 1–14. https://doi.org/10.2514/6.2014-3708.

[9] Huang, W., Kamhawi, H., Haag, T. W., Ortega, A. L., and Mikellides, I. G., "Facility effect characterization test of NASA's HERMeS hall thruster," *52nd AIAA/SAE/ASEE Joint Propulsion Conference, 2016*, Vol. AIAA-2016-, 2016. https://doi.org/10.2514/6.2016-4828.

[10] MacDonald-Tenenbaum, N., Pratt, Q., Nakles, M., Pilgram, N., Holmes, M., and Hargus, W., "Background pressure effects on ion velocity distributions in an spt-100 hall thruster," *Journal of Propulsion and Power*, Vol. 35, 2019, pp. 403–412. https://doi.org/10.2514/1.B37133.

[11] Cusson, S. E., Dale, E. T., Jorns, B. A., and Gallimore, A. D., "Acceleration Region Dynamics in a Magnetically Shielded Hall Thruster," *Physics of Plasmas*, Vol. 26, 2019. https://doi.org/10.1063/1.5079414.

[12] Huang, W., and Kamhawi, H., "Facility Effects on the Ion Characteristics of a 12.5-Kilowatt Hall Thruster," *Journal of Propulsion and Power*, 2023, pp. 1–10. https://doi.org/10.2514/1.B39034.

[13] Myers, R., and Manzella, D., "Stationary Plasma Thruster Plume Characteristics," *International Electric Propulsion Conference*, 1993, p. 096.

[14] Manzella, D., and Sankovic, J., "Hall thruster ion beam characterization," *31st Joint Propulsion Conference and Exhibit*, American Institute of Aeronautics and Astronautics, 1995. https://doi.org/10.2514/6.1995-2927.

[15] Azziz, Y., "Experimental and theoretical characterization of a Hall thruster plume," Ph.D. thesis, Massachusetts Institute of Technology, 2007.

[16] Brown, D. L., Walker, M. L. R., Szabo, J., Huang, W., and Foster, J. E., "Recommended Practice for Use of Faraday Probes in Electric Propulsion Testing," *Journal of Propulsion and Power*, Vol. 33, 2017, pp. 582–613. https://doi.org/10.2514/1.B35696.

[17] Goebel, D. M., and Katz, I., *Fundamentals of Electric Propulsion*, Wiley, 2008. https://doi.org/10.1002/9780470436448.

[18] Katz, I., Jongeward, G., Davis, V., Mandell, M., Mikellides, I., Dressler, R., Boyd, I., Kannenberg, K., Pollard, J., and King, D., "A Hall effect thruster plume model including large-angle elastic scattering," *37th Joint Propulsion Conference and Exhibit*, American Institute of Aeronautics and Astronautics, 2001. https://doi.org/10.2514/6.2001-3355.

[19] Mikellides, I. G., Katz, I., Kuharski, R. A., and Mandell, M. J., "Elastic Scattering of Ions in Electrostatic Thruster Plumes," *Journal of Propulsion and Power*, Vol. 21, 2005, pp. 111–118. https://doi.org/10.2514/1.5046.

[20] Pullins, S., Chiu, Y.-H., Levandier, D., and Dressler, R., "Ion dynamics in Hall effect and ion thrusters - Xe(+) + Xe symmetric charge transfer," *38th Aerospace Sciences Meeting and Exhibit*, American Institute of Aeronautics and Astronautics, 2000. https://doi.org/10.2514/6.2000-603.

[21] Miller, J. S., Pullins, S. H., Levandier, D. J., hui Chiu, Y., and Dressler, R. A., "Xenon charge exchange cross sections for electrostatic thruster models," *Journal of Applied Physics*, Vol. 91, 2002, pp. 984–991. https://doi.org/10.1063/1.1426246.

[22] Hofer, R. R., and Gallimore, A. D., "Recent Results From Internal and Very-Near-Field Plasma Diagnostics of a High Specific Impulse Hall Thruster," *28th International Electric Propulsion Conference*, 2003, p. 037.

[23] Huang, W., Shastry, R., Herman, D. A., Soulas, G. C., and Kamhawi, H., "A New Method for Analyzing Near-Field Faraday Probe Data of Hall Thrusters," *49th AIAA/ASME/SAE/ASEE Joint Propulsion Conference*, American Institute of Aeronautics and Astronautics, 2013. https://doi.org/10.2514/6.2013-4118.

[24] Kamhawi, H., Haag, T., Huang, W., Yim, J., Herman, D. A., Peterson, P. Y., Williams, G., Gilland, J., Hofer, R. R., and Mikellides, I. G., "Performance, Facility Pressure Effects, and Stability Characterization Tests of NASA's 12.5-kW Hall Effect Rocket with Magnetic Shielding Thruster," *52nd AIAA/SAE/ASEE Joint Propulsion Conference*, American Institute of Aeronautics and Astronautics, 2016. https://doi.org/10.2514/6.2016-4826.

[25] Huang, W., Williams, G. J., Peterson, P. Y., Kamhawi, H., Gilland, J. H., and Herman, D. A., "Plasma Plume Characterization of the HERMeS During a 1722-hr Wear Test Campaign," *35th International Electric Propulsion Conference*, 2017.